

# Cluster-glass percolative scenario in $\text{CeNi}_{1-x}\text{Cu}_x$ studied by very low-temperature ac susceptibility and dc magnetization

N. Marcano,<sup>1,\*</sup> J. C. Gómez Sal,<sup>1</sup> J. I. Espeso,<sup>1</sup> L. Fernández Barquín,<sup>1</sup> and C. Paulsen<sup>2</sup>

<sup>1</sup>*Departamento CITIMAC, Universidad de Cantabria, 39005 Santander, Spain*

<sup>2</sup>*MCBT, Institut Néel, CNRS, 38042 Grenoble, France*

(Received 3 August 2007; revised manuscript received 17 October 2007; published 19 December 2007)

Measurements of the ac susceptibility and dc magnetization on intermetallic alloys of  $\text{CeNi}_{1-x}\text{Cu}_x$  ( $x=0.6, 0.5,$  and  $0.1$ ) down to very low temperature ( $\sim 100$  mK) are reported. The data show that a cluster-glass state is formed at a freezing temperature  $T_f$ . The dynamics of the  $x=0.1$  alloy can be well accounted for by simple thermal activation indicating weak interactions between the clusters. On the other hand, for  $x=0.6$  and  $0.5$  concentrations, the data near the freezing temperature are best fitted to a critical slowing down process characterized by the dynamic exponents  $z\nu\sim 8$  and  $\beta\sim 0.7$ . The zero field cooled and field cooled magnetization curves show irreversibility above the freezing temperature which indicates the presence of an inhomogeneous dynamic magnetic state in the range  $T_f < T < T_{ir}$ . No anomalies related to the onset of the ferromagnetic state are detected below the freezing point in any of the alloys. A staircaselike behavior is observed in the very low temperature ( $T < 500$  mK) hysteresis loops of the ferromagnetic alloys and is field dependent. The discreet jumps are due to the existence of mesoscopic domainlike avalanches. All these findings shed light on the dynamical nature of the cluster-percolative scenario proposed for these series.

DOI: [10.1103/PhysRevB.76.224419](https://doi.org/10.1103/PhysRevB.76.224419)

PACS number(s): 71.27.+a, 75.40.Gb, 75.50.Lk, 75.60.Ej

## I. INTRODUCTION

Intermetallic  $3d$ - $4f$  magnetic compounds with substitutions on the magnetic or nonmagnetic sites present, not only the original difficulty of considering the competition among magnetic interactions (i.e., Ruderman-Kittel-Kasuya-Yosida (RKKY),  $4f$ - $3d$  hybridization, crystal electric field, etc.) but also an additional troublesome ingredient due to the disorder coming from the substitution effects.<sup>1,2</sup> In most cases, these effects are intrinsic to the samples and cannot be avoided by means of different preparation methods or supplementary thermal treatments. The simultaneous existence of competing interactions and disorder can give rise to short-range order or to a rich variety of magnetic behaviors related to clustered magnetic states. The latter are manifest by puzzling effects such as spin-glass phases,<sup>3</sup> superparamagnetism,<sup>4</sup> cluster glass,<sup>5</sup> or magnetic phase coexistence.<sup>6</sup>

The way to distinguish between these magnetic states has been discussed over the years, yet in many cases, the criteria to define the different states are not well established.<sup>7</sup> The difficulty arises from the dynamic magnetic character of most of these clustered systems, and thus, the temporal window of the probe used for the experimental study is crucial to achieve a proper understanding of the novel effects. Among the macroscopic techniques, ac susceptibility is one of the best suited to evaluate such a dynamic character. This is due to its intrinsic sensitivity (related to its inherent derivative nature) to detect very subtle magnetic transitions and/or different magnetic phases. Furthermore, ac susceptibility allows probing much longer times [usually between  $10^2$  and  $10^{-3}$  s in a superconducting-quantum-interference-device (SQUID)-based susceptometer] than powerful microscopic techniques such as neutron<sup>8</sup> ( $\tau_{\text{neutron}}$  between  $10^{-11}$  and  $10^{-14}$  s) and muon spectroscopies<sup>9</sup> ( $\tau_{\text{muon}}$  between  $10^{-8}$  and  $10^{-11}$  s) for the same sample and under identical conditions. In addition, a biasing  $H_{dc}$  field can be simultaneously applied. The use of

identical measuring conditions is relevant when dealing with samples which depend on the magnetic history (the latter being important for materials with magnetic irreversibility).

Within this context, one of the best examples of a complex magnetic behavior arising from substitution effects is the  $\text{CeNi}_{1-x}\text{Cu}_x$  system. The use of combined macroscopic and microscopic techniques has been crucial to propose a complete phenomenological model able to describe the puzzling experimental results obtained from the different techniques. In a recent report on the specific heat study<sup>10</sup> and considering previous magnetization,<sup>11</sup> neutron,<sup>12,13</sup> and muon spectroscopy<sup>14</sup> ( $\mu\text{SR}$ ) results, we proposed a tentative description of the magnetic behavior of the series. This has been very recently confirmed using small angle neutron scattering (SANS) data, allowing to establish a percolative model which connects the cluster-glass state observed at high temperatures with the long-range ferromagnetic ordered state at lower temperatures, observed by neutron diffraction for  $T < 100$  mK.<sup>15</sup> As temperature is decreased from the paramagnetic state, where the magnetic spins fluctuate freely, clusters develop due to the rise of short-range magnetic interactions. The temperature corresponding to the formation of the clusters ( $T^*$ ) coincides with the upper boundary of the intermediate state (consisting of ordered and nonordered phases) detected by  $\mu\text{SR}$ . The volume fraction of these dynamic entities increases as temperature is lowered and they become frozen at a characteristic temperature  $T_f$ . As commented above, the presence of clusters below  $T_f$  has been confirmed by SANS showing a correlation length of  $\sim 3$  nm.<sup>15</sup> Just below such a temperature, magnetic correlations are large enough to be considered as long-range order by  $\mu\text{SR}$  but not by neutron diffraction, where the ferromagnetic contribution to the intensity in the diffraction patterns is not observed until very low temperature of  $\sim 100$  mK ( $T \ll T_f$ ).<sup>12,13</sup> Thus, the studies carried out so far point toward the existence of a clustered state acting as a precursor of the

long-range ferromagnetic order. In this way, recent theoretical calculations<sup>16</sup> provide an interesting approach to the general phase diagram of the  $\text{CeNi}_{1-x}\text{Cu}_x$  series.

Preliminary measurements consisting of ac susceptibility ( $\chi_{ac}$ ) and dc magnetization ( $M_{dc}$ ) only down to 2 K were carried out in some representative compositions of the series ( $0.2 < x < 0.6$ ) (Ref. 17), indicating a freezing temperature  $T_f$  characteristic of a spin-glass-like state. However, the proximity of  $T_f$  to the experimental temperature limit (1.9 K) hardly allowed us to define a proper maximum in  $\chi_{ac}$ , and in some cases (i.e.,  $x \sim 0.2$ ), only an upturn could be observed near 2 K. Thus, it is necessary to extend the ac susceptibility and dc magnetization studies down to a very low-temperature range ( $T \ll T_f$ ) in some representative ferromagnetic compositions of the series ( $x=0.6, 0.5$ ) in order to explore the temperature regime between the well-characterized ferromagnetic state and the reported cluster-glass state. In addition, in order to get a complete understanding of the magnetic phase diagram reported on the  $\text{CeNi}_{1-x}\text{Cu}_x$ ,<sup>11</sup> we will pay particular attention to the compositional region near the magnetic-nonmagnetic crossover ( $x \sim 0.2$ ) where only preliminary results based on magnetization were reported.<sup>18</sup> By contrast, the Cu-rich compounds ( $x=1, 0.9$ ) have not been included in the present study since they are conventional antiferromagnets without any trace of spin-glass behavior.<sup>11</sup>

## II. EXPERIMENTAL DETAILS

The samples in the present work are those with  $x=0.6, 0.5, 0.4$ , and  $0.1$ . They are all polycrystalline samples prepared by carefully melting together stoichiometric amounts of the appropriate high-purity starting elements in an arc-melting furnace under inert Ar atmosphere. Five consecutive melts were performed flipping the arc-melted sample disk between melts, in order to improve homogeneity. The sample quality was checked at room temperature by x-ray diffraction and scanning electron microscopy. The crystalline structure of the  $\text{CeNi}_{1-x}\text{Cu}_x$  compounds studied has been determined by x-ray diffraction at 300 K. The alloys with  $x > 0.15$  crystallize in the FeB-type orthorhombic structure ( $Pnma$  space group), whereas those with  $x \leq 0.15$  crystallize in the CrB-type orthorhombic structure ( $Cmcm$  space group). The details about the preparation, crystallography, and quality control of the samples have previously been reported.<sup>10</sup>  $\chi_{ac}$  (and the frequency dependence) and low-field magnetization in field cooled (FC) and zero field cooled (ZFC) were measured down to 80 mK using a SQUID magnetometer equipped with a miniature dilution refrigerator at the MCBT, Institut Néel in Grenoble (formerly the CRTBT). High-field magnetization measurements were carried out up to 40 kOe at 300 mK on  $\text{CeNi}_{0.5}\text{Cu}_{0.5}$  and up to the same field at 100 mK on  $\text{CeNi}_{0.9}\text{Cu}_{0.1}$ .  $\chi_{ac}$  measurements were performed in the frequency range of  $0.021 \leq \omega/2\pi \leq 111$  Hz. The amplitude of the ac field used in this study was  $h_{ac}=1$  Oe. For some particular cases, field dependent of ac measurements up to 1 kOe and down to 1.8 K has been performed with a Quantum Design Physical Property Measurement System (PPMS) magnetometer from at the University of Cantabria.

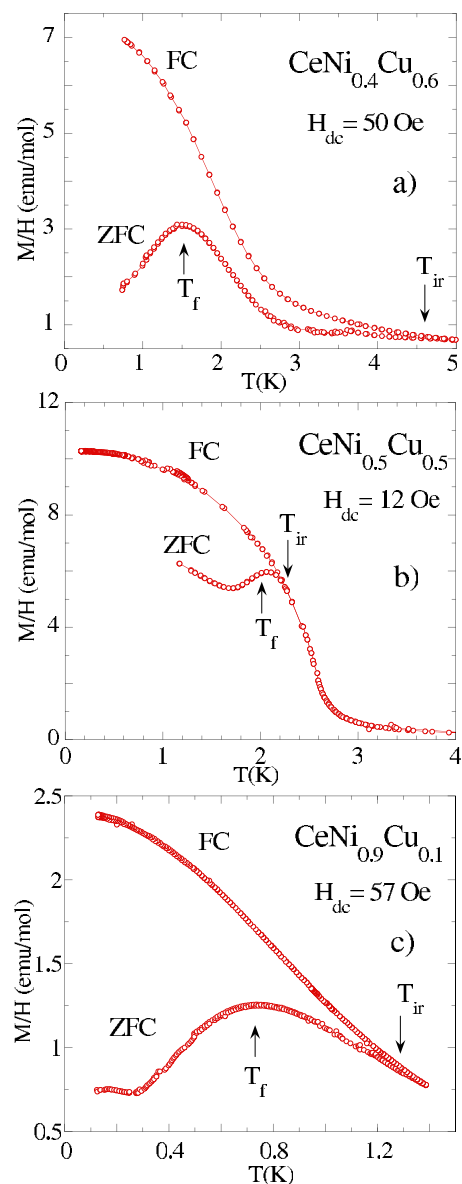


FIG. 1. (Color online) Field cooled and zero field cooled dc magnetization as a function of temperature for (a)  $\text{CeNi}_{0.4}\text{Cu}_{0.6}$  with a field of 50 Oe, (b)  $\text{CeNi}_{0.5}\text{Cu}_{0.5}$  with a field of 12 Oe, and (c)  $\text{CeNi}_{0.9}\text{Cu}_{0.1}$  with a field of 57 Oe. Continuous lines drawn are guides to the eye. Note the different scales in temperature.

## III. RESULTS

Figure 1 shows the temperature variation of the dc susceptibility ( $\chi=M/H$ ) of  $\text{CeNi}_{0.4}\text{Cu}_{0.6}$ ,  $\text{CeNi}_{0.5}\text{Cu}_{0.5}$ , and  $\text{CeNi}_{0.9}\text{Cu}_{0.1}$  measured in the FC and ZFC modes for low magnetic fields. In all the cases, the zero field cooled susceptibility ( $\chi_{ZFC}$ ) shows a broad maximum at  $T_f$  as well as the appearance of irreversibility which is manifest as a bifurcation between the ZFC and FC curves below a characteristic temperature  $T_{ir}$  (see Table I). It should be noted that in the case of canonical spin glasses, the onset of the irreversibility ordinarily starts very close to, but slightly below,  $T_f$ ,<sup>5,7</sup> whereas in the present case, it occurs well above this temperature. Another distinct feature with respect to canonical

TABLE I. Magnetic properties of  $\text{CeNi}_{1-x}\text{Cu}_x$  obtained from the analysis of ac-dc susceptibility: effective magnetic moment ( $\mu_{eff}$ ) per Ce atom and the paramagnetic Curie temperature ( $\theta_p$ ) obtained from the fit of the reciprocal susceptibility curve to the Curie-Weiss law (Refs. 18 and 22), the irreversibility temperature which marks the bifurcation of  $\chi_{ZFC}$  and  $\chi_{FC}$  dc magnetization curves ( $T_{ir}$ ), spin freezing temperature ( $T_f$ ) (at the lowest frequency), frequency shift of freezing temperature ( $\delta$ ), activation energy ( $E_a$ ), characteristic relaxation time obtained from thermal activation  $\tau_0$ , glass transition temperature ( $T_g$ ) (at  $\omega \rightarrow 0$ ), critical exponents ( $z\nu$ ) and ( $\beta$ ), characteristic relaxation time obtained from critical slowing down analysis  $\tau_0^*$ , the remanent moment ( $M_r$ ), and the coercive field ( $H_c$ ) from hysteresis loops at temperatures well below  $T_f$  ( $T=100$  mK for  $x=0.1$  and  $T=300$  mK for  $x=0.5$  and  $T=500$  mK for  $x=0.6$ ).

$x$	$\mu_{eff}$ ( $\mu_B$ )	( $\theta_p$ ) (K)	$T_{ir}$ (K)	$T_f$ (K)	$\delta$	$E_a$ (K)	$\tau_0$	$z\nu$	$\beta$	$\tau_0^*$	$T_g$ (K)	$M_{rem}$ ( $\mu_B/\text{Ce at.}$ )	$H_c$ (kOe)
0.1	2.4	-60	1.3	0.91(2)	0.062(1)	20(1)	$2 \times 10^{-13}$					0.035	0.70
0.5	2.4	-14	2.3	2.21(2)	0.013(1)			7.3	0.70(5)	$4 \times 10^{-11}$	2.10	0.08	0.15
0.6	2.4	-10	4.5	1.74(2)	0.010(2)			7.4	0.70(5)	$5 \times 10^{-13}$	1.70	0.24	0.35

spin glasses is that  $\chi_{FC}$  continues to increase below  $T_f$ , resembling cluster-glass behavior. This kind of behavior has been reported in various metallic systems (amorphous DyNi),<sup>19</sup> reentrant spin-glass insulating systems ( $\text{La}_{0.5}\text{Sr}_{0.5}\text{CoO}_3$ ),<sup>20</sup> and the electron-doped manganite  $\text{Ca}_{1-x}\text{Sm}_x\text{MnO}_3$ ,<sup>21</sup> among others.

The in-phase  $\chi'_{ac}(\omega, T)$  and the out-of-phase  $\chi''_{ac}(\omega, T)$  components of the ac susceptibility measured at various frequencies  $f = \omega/2\pi$  are shown in Fig. 2 plotted against the temperature for  $\text{CeNi}_{0.4}\text{Cu}_{0.6}$  and  $\text{CeNi}_{0.5}\text{Cu}_{0.5}$ . These alloys are representative of those presenting long-range ferromagnetic order at very low temperature.<sup>13</sup> Both  $\chi'_{ac}(\omega, T)$  and  $\chi''_{ac}(\omega, T)$  curves show a pronounced maximum whose ampli-

tude and position depend on the frequency of the applied ac magnetic field. The position of the maxima shifts to higher temperature and the amplitude decreases with increasing frequency. An example of an alloy with low Cu substitutions (and which does not exhibit long-range ferromagnetic order at low temperature) is presented in Fig. 3  $\chi'_{ac}(\omega, T)$  for  $\text{CeNi}_{0.9}\text{Cu}_{0.1}$ . In addition to the frequency dependence of the maxima in  $\chi'_{ac}(\omega, T)$ , this figure also shows that the anomaly is strongly reduced by the application of a weak superimposed magnetic field ( $H_{dc} = 1$  kOe), which is a common feature of all the studied compounds.<sup>11</sup>

A quantitative measure of the effect of the frequency in shifting the peak in  $\chi'_{ac}$  is given by  $\delta = \Delta T_f / (T_f \Delta \ln \omega)$  which allows us to compare the  $\omega$  dependence of  $T_f$  in different systems. The observed values are displayed in Table I. We find  $\delta$  values ranging from 0.062 for  $x=0.1$  to 0.010 for  $x=0.6$ . These values are intermediate between those reported for canonical spin glasses ( $\delta \sim 0.005$ ) (Ref. 7) and those reported for noninteracting ideal superparamagnetic systems ( $\delta \sim 0.1$ ).<sup>4</sup> Thus, the behavior of our system best corresponds to an intermediate situation, the so-called cluster glass, usually interpreted as an ensemble of interacting magnetic clusters randomly arranged and sometimes characterized as reen-

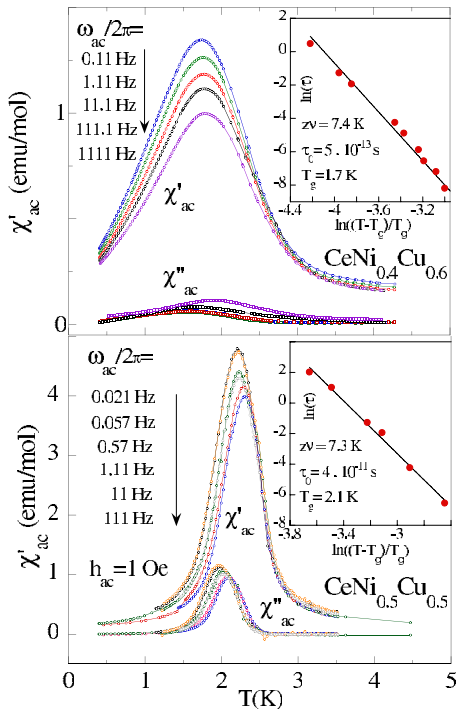


FIG. 2. (Color online) The real ( $\chi'_{ac}$ ) and imaginary ( $\chi''_{ac}$ ) components of the ac susceptibility as a function of temperature in an applied ac field of 1 Oe at various selected frequencies for  $\text{CeNi}_{0.4}\text{Cu}_{0.6}$  (top panel) and  $\text{CeNi}_{0.5}\text{Cu}_{0.5}$  (bottom panel). The inset shows the critical slowing down analysis in each case. The line corresponds to the best fitting (see text for details).

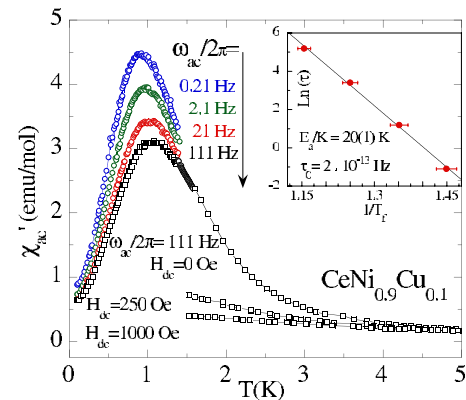


FIG. 3. (Color online) The real ( $\chi'_{ac}$ ) component of the ac susceptibility in an applied ac field of 1 Oe at various selected frequencies for  $\text{CeNi}_{0.9}\text{Cu}_{0.1}$ . Figure also shows  $\chi'_{ac}$  at  $\omega/2\pi = 111$  Hz as a function of temperature measured at different applied fields (up to 1000 Oe) above 1.8 K. The inset shows the frequency dependence of  $T_f$  analyzed with the thermal activation law.

trant spin glasses.<sup>7,23</sup> Examples of  $\delta$  values of this magnitude can be found in other strongly correlated metallic systems such as  $\text{Ce}_2\text{AgIn}_3$  ( $\delta=0.022$ ),<sup>24</sup>  $\text{URh}_2\text{Ge}_2$  ( $\delta=0.025$ ),<sup>25</sup> and  $\text{U}_2\text{AuGa}_3$  ( $\delta=0.01$ ).<sup>26</sup> It should be recalled that such a frequency dependence for low values ( $\omega < 1000$  Hz) is not typically observed for the case of a second order transition with a well-defined ordering temperature  $T_C$  (FM) or  $T_N$  (AFM). For these phase transitions, frequencies ranging from megahertz to gigahertz are required to detect a shift in the maxima.<sup>7</sup>

Whenever a frequency shift is observed in the ac susceptibility, thermally activated processes can be invoked which can account for the presence of magnetization relaxation of clusters or small domains.<sup>27</sup> This can be evaluated using a simple law,

$$\tau = \tau_0 \exp\left[\frac{E_a}{kT_f}\right], \quad (1)$$

where  $\tau_0$  is related to the characteristic attempt frequency  $\omega_0 = \tau_0^{-1}$  of the clusters,  $E_a$  is the average activation energy barrier the clusters must overcome in order to align with the field, and  $k$  is the Boltzmann constant. The inset of Fig. 3 shows a fit of the data for  $x=0.1$  alloy to Eq. (1) plotted as  $\ln \tau$  vs  $1/T_f$  where  $\tau = 1/2\pi f$  and  $T_f$  are taken from the peaks in  $\chi''_{ac}$  for a given measuring frequency  $f$ . The slope of the linear fit gives an average energy barrier  $E_a = 20$  K and the intercept gives  $\tau_0 = 2 \times 10^{-13}$  corresponding to an  $\omega_0 = 5 \times 10^{13}$  (values reported in Table I). These values are very reasonable; typical magnitudes for  $\omega_0$  range from  $10^{10}$  to  $10^{13}$  Hz are observed in magnetic cluster systems,<sup>7</sup> and the barrier at 20 K is what one would expect for freezing near 1 K.

Similarly, fits of the peaks in the  $\chi''_{ac}$  data for  $x=0.5$  and  $0.6$  alloys were also made. However, the fits were rather poor, and more revealing, the parameters from the fits,  $\tau_0 = 2 \times 10^{-50}$ ,  $\tau_0 = 2 \times 10^{-60}$  and  $E_a = 220$  K,  $E_a = 300$  K (for  $x = 0.5$  and  $0.6$ , respectively), are unphysical. These results imply that there exists an evolution from the high-Cu concentration alloys to the very diluted  $x=0.1$  alloy; for the former, it is clear that magnetic intercluster interactions are definitely existing, whereas for the latter, the interactions are so weak that relaxation is macroscopically independent.

On the other hand, when interactions are present, ordering may occur and the dynamics may be better accounted for by critical slowing down as the system nears a phase transition. Indeed, do the nature of the RKKY interaction in the present system, as well as disorder due to random substitutions in the higher concentration alloys, one would expect competing interactions and frustration to be present, and a spin-glass transition to occur. One way to analyze the critical behavior in this process is to measure the divergence of the relaxation times  $\tau$  as the temperature approaches the critical temperature  $T_g$  at which the phase transition takes place. The conventional result of dynamical scaling relates the relaxation time for the decay of the fluctuations  $\tau$  to the spin correlation length  $\xi$  as  $\tau \propto \xi^z$ ,  $z$  being the dynamic critical exponent. Since  $\xi$  diverges with temperature as  $\xi \sim [T/(T-T_g)]^\nu$ , where  $\nu$  is a critical exponent, the expression for  $\tau$  is given by<sup>7</sup>

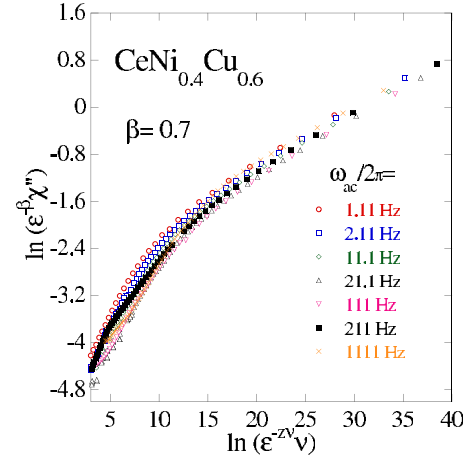


FIG. 4. (Color online) Critical slowing down analysis of the imaginary part of the ac magnetic susceptibility ( $\chi''_{ac}$ ) data at  $T > T_g$  for the  $\text{CeNi}_{0.4}\text{Cu}_{0.6}$  alloy.  $\chi''_{ac}$  at different frequencies of the ac field collapse on a master curve with  $\beta=0.7$ .

$$\tau = \tau_0^* \left(\frac{T}{T_g} - 1\right)^{-z\nu}, \quad (2)$$

in which  $T_g$  is the transition temperature,  $\tau_0^*$  is the characteristic relaxation time of the fluctuating entities, and  $z\nu$  is the dynamic critical exponent. Thus, if we assume conventional critical slowing down upon approaching  $T_g$  from above, the relaxation time is expected to obey the temperature dependence

$$\tau = \tau_0^* \left(\frac{T_f - T_g}{T_g}\right)^{-z\nu}, \quad (3)$$

where here  $T_f$  corresponds to the peak in  $\chi''_{ac}$  at a given measuring frequency  $f$  and  $\tau = 1/2\pi f$ .<sup>28</sup>  $T_g$  represents the infinitely slow cooling dc (equilibrium) value of  $T_f$  ( $\omega \rightarrow 0$ ).

The insets of Fig. 2 shows the data points and the straight lines are the results of a three parameter fit to Eq. (3), yielding values for  $\tau_0^*$ ,  $T_g$ , and  $z\nu$  given in Table I for  $x=0.5$  and  $0.6$  alloys. The  $\tau_0^*$  values fall within the range of other metallic spin-glass systems.<sup>29</sup> The  $z\nu$  value compares well with those reported on different spin-glass systems ( $5 < z\nu < 11$ ) as reviewed by Souletie and Tholence,<sup>30</sup> usually labeled as “fragile regime.” Overall, these values agree with the  $z\nu = 7.9$  obtained through calculations by Ogielski and Morgevstern for three-dimensional spin glasses with short-range magnetic interactions, in contrast to the expected value  $z\nu \approx 2$  in conventional phase transitions.<sup>31</sup> Finally,  $T_g$  for both samples are quite plausible.

In addition, a dynamic scaling of the imaginary part of the susceptibility  $\chi''$  is also expected to occur at a spin glass transition.<sup>32</sup> Letting  $\varepsilon = \frac{T-T_g}{T_g}$ , then

$$\chi''(\nu, T) = \varepsilon^\beta F(\nu\varepsilon)^{z\nu}. \quad (4)$$

Figure 4 shows the power-law scaling of  $\chi''_{ac}$  for  $\text{CeNi}_{0.4}\text{Cu}_{0.6}$ , as an example of the series. The scaling has been made using the value of  $T_g$  and  $z\nu$  obtained from the fits to Eq. (3). The result shows a convincing scaling using  $\beta$

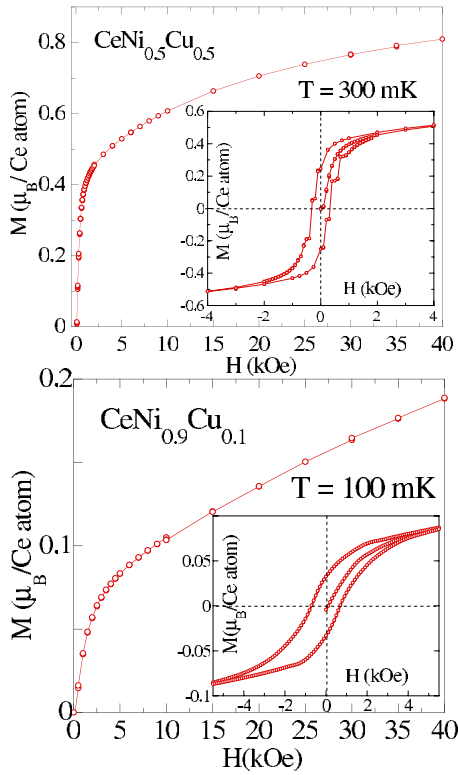


FIG. 5. (Color online) High-field magnetization  $M(H)$  up to 40 kOe for  $\text{CeNi}_{0.5}\text{Cu}_{0.5}$  obtained at  $T=300$  mK (top panel) and  $\text{CeNi}_{0.9}\text{Cu}_{0.1}$  obtained at  $T=100$  mK (bottom panel). Insets display the hysteresis loops measured at 300 and 100 mK, respectively. Continuous lines drawn are guides to the eye.

$=0.7$ , with all the branches collapsing onto a universal curve. This universal curve is as well obtained for the case of  $x=0.5$  compound with the same  $\beta$  value ( $\beta=0.70\pm 0.05$ ) (see Table I). These values are relatively close to the exponent ( $\beta=0.5$ ) obtained through Monte Carlo simulations.<sup>7</sup> Also, they are in the range of other intermetallic compounds and more recently  $\text{Y}_{0.6}\text{U}_{0.4}\text{Pd}_3$  ( $\beta=0.9$ ).<sup>33</sup>

Magnetization measurements as a function of field [ $M(H)$ ] at temperatures well below  $T_f$  show many pertinent features in these compounds. Figures 5(a) and 5(b) depict  $M(H)$  obtained under the ZFC condition up to 40 kOe for  $\text{CeNi}_{0.5}\text{Cu}_{0.5}$  at 300 mK, i.e., in the ferromagnetic regime detected by neutron diffraction, and for  $\text{CeNi}_{0.9}\text{Cu}_{0.1}$  at 100 mK. In both cases, there is a sharp rise at low fields ( $H_{dc} < 1$  kOe) followed by a monotonic increase in the high field range without reaching saturation. Furthermore, the absolute values of magnetization at high magnetic fields are below  $1\mu_B/\text{Ce at.}$ : For  $x=0.5$ , as an example, the highest value is  $0.8\mu_B/\text{Ce at.}$  at the highest field (40 kOe) which is far from saturation. This may be considered as another indication for the existence of cluster-glass behavior with a rather strong random anisotropy. In such a situation, the initial magnetization will be steep as clusters are at first saturated along their local easy axis. However, a much larger external field is needed in order to overcome the distribution of randomly oriented anisotropy axes before the various clusters can point along the field direction and become fully aligned.

The magnetization values for  $x=0.1$  obtained at 100 mK are much smaller than those found for the other compounds. In particular, the value of the magnetization at the highest field ( $M_{\text{max}}$ ) is  $\sim 0.2\mu_B/\text{Ce at.}$ , i.e., 22% of the value observed for  $x=0.5$ . This feature is in accordance with the enhancement of the 4f-conduction band hybridization (Kondo interaction), which strongly reduces the value of the magnetic moment in the  $x=0.1$  compound.

Hysteresis loops in the ZFC condition have been obtained well below  $T_f$  and provide useful information for the interpretation of the magnetic ground state of the system. Examples of the hysteresis loops are shown in the inset of Fig. 5 (top bottom) for  $x=0.5$  at  $T=300$  mK and for  $x=0.1$  at  $T=100$  mK, respectively. We observed that whereas for  $x=0.1$ , the loop is smooth, for  $x=0.5$  the reversal magnetization changes in a series of large discrete jumps. These jumps in the hysteresis loops have also been observed in other ferromagnetic compounds of the series (i.e.,  $x=0.4$ ) at very low temperatures. The latter alloy has been analyzed in detail in order to gain insight on this staircase-like behavior. Such an analysis is depicted in Fig. 6. The top panel displays two consecutive hysteresis loops obtained for  $\text{CeNi}_{0.6}\text{Cu}_{0.4}$  at  $T=100$  mK. In both loops, the magnetization changes in a series of large discrete jumps giving rise to a multistep pattern although the steps appear at different field values. These jumps are constricted to very low temperatures vanishing for slightly higher temperatures ( $T > 300$  mK), as shown in Fig. 6(b). Also, we find that the multistep pattern depends on the field spacing ( $\Delta H$ ). This is shown in Fig. 6(c) where at  $T=100$  mK the number of jumps in the magnetization curve and their position changes as the field spacing is increased. Finally, other loop characteristic parameters such as remanent magnetization  $M_r$  and the coercive field  $H_c$  are listed in Table I for the different samples of the series. The compound with the lowest Cu concentration ( $x=0.1$ ) presents the highest coercivity ( $H_c=0.7$  kOe) at 100 mK and the lowest remanence ( $M_r \sim 0.03\mu_B/\text{Ce at.}$ ) in the series.

#### IV. DISCUSSION

The static and dynamic susceptibility and magnetization data down to very low temperatures presented in this paper provide clear evidence for the existence of a cluster-glass state below a characteristic freezing temperature  $T_f$ . In summary we find (i) Irreversibility below  $T_{ir}$  ( $T_{ir} > T_f$ ), (ii) low-frequency shift of  $\chi'_{ac}$  and  $\chi''_{ac}$ , (iii) critical (dynamic) slowing down in the proximity of the characteristic glass temperature  $T_g$ , and (iv) lack of saturation of the high-field magnetization curves, suggestive of cluster-glass-like behavior. Furthermore, the striking multistep behavior in the hysteresis loops reinforces the picture of the clustered percolative magnetic state proposed.<sup>15</sup> The present study strongly supports this model because ac-dc magnetization measurements do not reveal any additional transition below  $T_f$ , in addition to providing quantitative parameters related to the freezing process.

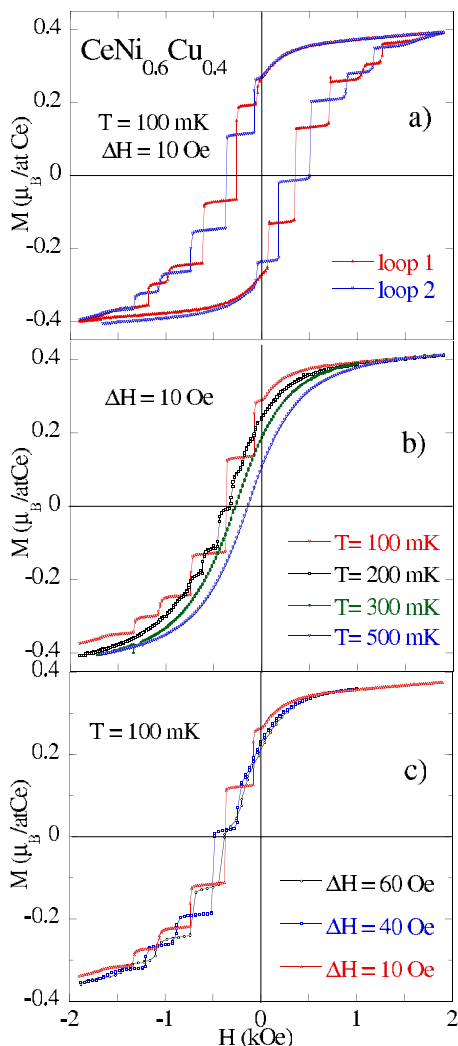


FIG. 6. (Color online) Hysteresis loops obtained for  $\text{CeNi}_{0.6}\text{Cu}_{0.4}$ : (a) two consecutive loops obtained at 100 mK with a field spacing  $\Delta H = 10$  Oe, (b) the decreasing field part of major hysteresis loops obtained at different temperatures between 100 and 500 mK at a fixed field spacing of 10 Oe, (c) the decreasing field part of major hysteresis loops obtained for different field spacings between 10 and 60 Oe at a fixed temperature  $T = 100$  mK.

We first consider the ZFC and FC curves, the bifurcation of which takes place at a characteristic temperature  $T_{ir}$  above the maximum in the ZFC curve ( $T_f$  as defined by  $\chi'_{ac}$ )—unexpected in a spin glass. Especially in  $x = 0.6$  alloy, the value of  $T_{ir}$  far exceeds  $T_f$  ( $T_{ir} \sim 2.6T_f$ ). Here,  $T_{ir}$  corresponds to the characteristic temperature defined by  $\mu\text{SR}$  spectroscopy, which defines the establishment of an intermediate inhomogeneous magnetic state in the temperature range  $T_f < T < T_{ir}$ .<sup>14</sup> Such a state corresponds to the presence of dynamic entities that progressively lose their dynamical behavior to finally freeze at  $T_f$ .

The results of the ac susceptibility clearly show a transition presenting a critical slowing down process for the stronger ferromagnetic compositions ( $x = 0.6, 0.5$ ). This is reflected by the  $z\nu$  and  $\beta$  values obtained for these two alloys

( $z\nu = 7.4$  and  $\beta = 0.7$  for  $x = 0.6$  and  $z\nu = 7.3$  and  $\beta = 0.7$  for  $x = 0.5$ ) which are in the range of the spin-glass systems. Remarkably, the spin relaxation time distribution is significantly different between both alloys, since the anomaly in  $\chi'_{ac}$  for  $x = 0.5$  ( $\text{FWHM}_{x=0.5} \sim 1$  K) is much narrower than  $x = 0.6$  ( $\text{FWHM}_{x=0.6} \sim 2.5$  K). This is a sign of a more collective process taking place in  $x = 0.5$ . In contrast, the analysis indicate a collection of clusters with different relaxation times behaving more independently in the alloy with a lower concentration of Cu ( $x = 0.1$ ). This results in the large  $\delta$  value and thermally activated process, without critical slowing down.

Following with the compositional analysis, the magnetization measurements reveal additional information about the percolative and coupling processes among the clusters. In  $x = 0.5$  alloy, the ZFC-FC branches are relatively close, and the ZFC curve presents a large magnetic response for  $T < 2$  K, which is different from the behavior observed in  $x = 0.6$  alloy. A small field of  $H_{dc} = 12$  Oe for  $x = 0.5$  is enough to trigger the ferromagnetic correlations among the clusters. This is probably due to the existence of a weak magnetic disordered interface which allows the ferromagnetic coupling. In the case of  $x = 0.6$ , the magnetic response is smaller in spite of using a five times larger in magnitude magnetic field. This would indicate that the clusters are more isolated with a thicker disordered interface.<sup>34</sup> On the other hand, the presence of such ferromagnetic clusters accounts for the continuous rise of FC magnetization with decreasing temperature below  $T_f$ . Similar behavior has been also reported for some random anisotropy systems,<sup>19</sup> exhibiting a complex magnetic arrangement termed “speromagnetism.”<sup>35</sup> In those systems, the competition between magnetic exchange interactions and the local magnetic anisotropy plays a crucial role in determining the shape of the FC branch. In similar fashion, our experimental data indicate strong random anisotropy in the clustered state of these alloys. The strengthening of the intercluster coupling is also indicated by the dynamics of the cluster relaxation: The  $x = 0.1$  alloy is on the verge of ferromagnetism since Ce magnetic moment is strongly reduced owing to an appreciable Kondo effect near CeNi. The very weak coupling of the magnetic clusters in this alloy results in a totally different dynamic process than corresponding to both  $x = 0.5$  and  $0.6$  alloys as we point out above.

The magnetization as a function of field at very low temperatures also supports the previous finding:  $\chi_{lf}(x = 0.5) \sim 10\chi_{lf}(x = 0.1)$  in the low magnetic field range of 0–1 kOe, indicating stronger ferromagnetic correlations in  $x = 0.5$  although the curves were recorded at different temperatures. In the case of the high-field magnetization, we find  $\chi_{hf}(x = 0.5) \sim 3\chi_{hf}(x = 0.1)$  for the magnetic field range of 20–40 kOe, signaling stronger magnetic moment canting in  $x = 0.5$  alloy where the clusters are well formed. Moreover, the smaller coercive field  $H_c = 0.15$  kOe of  $x = 0.5$  alloy indicates stronger correlations between clusters than  $x = 0.1$  alloy ( $H_c = 0.7$  kOe).

The hysteresis loops of the analyzed ferromagnetic compositions show staircaselike behavior at very low temperatures with the following chief characteristics: (i) the jumps

occur at different values of the external magnetic field for different runs, (ii) they appear in the reversal magnetization of the loop whereas the first magnetization curve appears smooth and devoid of jumps, (iii) the steps are dependent on the field spacing, and (iv) they appear at very low temperatures ( $T \ll T_f$ ), vanishing for a slight increase of the temperature.

Patterns of discreet and sharp jumps in the magnetization curves have been reported in very different systems over the last years, from the simplest system as molecular chains of magnetic spins<sup>36</sup> to extremely complex perovskite oxides where phase separation, charge, and spin ordering have been discussed.<sup>37</sup> Different mechanisms have been proposed to describe the experimental findings. In some cases, steps are observed at regular field intervals and have been interpreted as evidence of thermally assisted, field-tuned resonant tunneling between quantum spin states. This interpretation has been applied to systems involving a large number of identical high-spin molecules, as in the case of Mn<sub>12</sub> acetate<sup>38</sup> and the so-called Fe<sub>8</sub> (Ref. 36) clusters, among others. In those cases, the step fields are true critical fields, and thus, they should be reproducible in contrast with the finding in our alloys with a spin structure radically different from molecular magnets. Nonrepetitive jumps, similar to our observation, have been reported for some phase-separated manganese oxides<sup>39</sup> for which a martensitic origin was invoked. The jumps, however, were observed in the first magnetization curve at much higher fields ( $H > 10$  kOe at temperatures around 2 K in that particular case), being absent in the smooth return branch.

Another mechanism that can lead to jumps is the presence of random fields. Under this mechanism, an external field flips a given domain thereby reversing the magnetization of the neighboring domains, thus leading to an avalanche of flipping domains. Such a scenario has been proposed in disordered systems such as the amorphous Dy-Cu (Ref. 40) and, more recently, in the single crystal antiferromagnet PrVO<sub>3</sub>.<sup>41</sup> Although the particular microscopic origin leading to this situation is different from our case, the qualitative description of this mechanism is able to account for our experimental results in the hysteresis loops [described from (i) to (iv)]. In the proposed percolative cluster-glass model,<sup>15</sup> the observed features in the loops are the mesoscopic analog of the Barkhausen noise. In fact, the magnetic domains appear in conventional ferromagnets in order to minimize the magnetostatic energy. In the case of CeNi<sub>1-x</sub>Cu<sub>x</sub>, which comprises ferromagnetic clusters below  $T_f$ , domains arise due to thermally activated percolation of the static ferromagnetic clusters as they approach a minimum energy state. This process is driven by the increasing importance of the RKKY interaction as the temperature decreases. Monte Carlo simulations incorporating disorder, anisotropy, and competing magnetic interactions within this phenomenological model satisfactorily reproduce the experimental data.<sup>15,42</sup> Evidence therefore suggests that the formation of clusters with different anisotropy directions is at the origin of the staircaselike behavior in the hysteresis loops. Such a scenario provides an explanation for the absence of discreet jumps in  $x=0.1$  alloy at the lowest recorded temperature (100 mK): in this case, the interactions among the clusters are very weak, with a relatively

low  $T_f$  (0.9 K). At 100 mK, the size of the magnetic clusters is not big enough to yield ferromagnetic Bragg diffraction,<sup>13</sup> and thus, the domainlike structure observed in the ferromagnetic compositions is not achieved in this case.

Similar physics of domain avalanches have been recently reported in other systems showing staircase-like behavior. For instance, the superconducting ferromagnetic UGe<sub>2</sub> (Ref. 43) exhibits a step pattern dependent on the sample size and the measuring conditions. In addition, recent studies on cerium-doped and yttrium-doped manganites La<sub>0.67-x</sub>A<sub>x</sub>Ca<sub>0.33</sub>MnO<sub>3</sub> ( $A=\text{Ce, Y}$ ) reported a nonrepetitive multistep structure of Barkhausen-like jumps in the low-field region (up to 50 Oe), appearing also in the reversal magnetization.<sup>44</sup> In such a case, a picture of a soft ferromagnetic material with embedded clusters has been proposed, where mixed ferromagnetic and antiferromagnetic interactions compete. This picture is relatively close to our situation, since a heterogeneous clustered magnetic environment is intrinsically required for the existence of the staircase behavior.

## V. CONCLUSIONS

We have studied the magnetic properties of CeNi<sub>1-x</sub>Cu<sub>x</sub> alloys down to very low temperatures by means of static and dynamic magnetic susceptibilities. The present data show features of a ferromagnetic cluster-glass behavior in these compounds although particular dynamical processes can be distinguished for each composition. Whereas for the ferromagnetic alloys ( $x=0.6, 0.5$ ), we can define a freezing temperature reached by a critical slowing down process, the dynamics of the relaxation in the alloy with minor Cu substitution ( $x=0.1$ ) reflects that of a collection of clusters with weaker interactions as deduced from the high  $T_f$  shift and the absence of critical dynamics.

Measurements of the dc magnetization provide information about the percolative and coupling processes among the clusters in the studied alloys. The irreversibility observed in the low-field FC and ZFC magnetization curves above  $T_f$  is related to the formation of magnetic (dynamic) clusters in these compounds. The staircaselike behavior observed in the hysteresis loops at very low temperatures, which has been interpreted as the mesoscopic analog of the Barkhausen noise, strongly confirms the percolative cluster scenario proposed for this series.

We have discussed the observed results on the basis of the proposed cluster percolative mechanism in which variations in the substitutional disorder lead to a spread in the interfacial coupling of the clusters. The present results, considering also previous neutron scattering, heat capacity, and  $\mu$ SR data, allow us to revisit the magnetic phase diagram previously reported<sup>11</sup> in this series. The data reveal the formation of long-range ferromagnetic order below the cluster-glass transition without any indication of a sharp transition at a Curie temperature. Thus, the border defining the ferromagnetic state could not be exactly determined. This system represents a useful example of interacting magnetic clusters in the intermediate range between canonical spin glasses and Kondo-impurity metallic systems, as described by Mydosh.<sup>7</sup>

## ACKNOWLEDGMENTS

We would like to thank J. Rodríguez Fernández (U. Cantabria), G. M. Kalvius (T. U. Munich), J. R. Iglesias (U. F. Rio Grande, Brazil), and P. Haen (CRTBT, Grenoble) for

helpful discussions. E. Lhotel (CEA, Grenoble) is acknowledged for support with the SQUID measurements. This work is supported by the Spanish CICYT grant MAT2005-06806-C04-02 and the ECOM COST Action P16. N.M. acknowledges the Spanish MEC for financial support.

- 
- \*Present address: Cavendish Laboratory, University of Cambridge, Cambridge CB3 0HE, United Kingdom; nm382@cam.ac.uk
- <sup>1</sup>A. J. Millis, *Solid State Commun.* **126**, 3 (2003).
  - <sup>2</sup>E. Miranda and V. Dobrosavljevic, *Rep. Prog. Phys.* **68**, 2337 (2005).
  - <sup>3</sup>S. G. Magalhaes, F. M. Zimmer, and B. Coqblin, *J. Phys.: Condens. Matter* **18**, 3479 (2006).
  - <sup>4</sup>J. L. Dormann, L. Bessais, and D. Fiorani, *J. Phys. C* **21**, 2015 (1988).
  - <sup>5</sup>K. Binder and A. P. Young, *Rev. Mod. Phys.* **58**, 801 (1986).
  - <sup>6</sup>See, for instance, E. Dagotto, in *Nanoscale Phase Separation and Colossal Magnetoresistance* (Springer-Verlag, Berlin, 2002).
  - <sup>7</sup>J. A. Mydosh, *Spin Glasses: An Experimental Introduction* (Taylor & Francis, London, 1993).
  - <sup>8</sup>See, for instance, M. F. Hansen, F. Bødker, S. Mørup, K. Lefmann, K. N. Clausen, and P.-A. Lindgård, *Phys. Rev. Lett.* **79**, 4910 (1997); D. N. Argyriou, J. W. Lynn, R. Osborn, B. Campbell, J. F. Mitchell, U. Ruett, H. N. Bordallo, A. Wildes, and C. D. Ling, *ibid.* **89**, 036401 (2002); H. Casalta, P. Schleger, C. Bellouard, M. Hennion, I. Mirebeau, G. Ehlers, B. Farago, J.-L. Dormann, M. Kelsch, M. Linde, and F. Phillipp, *ibid.* **82**, 1301 (1999).
  - <sup>9</sup>G. M. Kalvius, D. R. Noakes, and O. Hartmann, *Handbook on the Physics and Chemistry of Rare Earths* (North-Holland, Amsterdam, 2001), Vol. 32, pp. 55–451.
  - <sup>10</sup>N. Marcano, J. I. Espeso, J. C. Gómez Sal, J. Rodríguez Fernández, J. Herrero-Albillos, and F. Bartolomé, *Phys. Rev. B* **71**, 134401 (2005).
  - <sup>11</sup>J. García Soldevilla, J. C. Gómez Sal, J. A. Blanco, J. I. Espeso, and J. Rodríguez Fernández, *Phys. Rev. B* **61**, 6821 (2000).
  - <sup>12</sup>J. I. Espeso, J. García Soldevilla, J. A. Blanco, J. Rodríguez Fernández, J. C. Gómez Sal, and M. T. Fernández, *Eur. Phys. J. B* **18**, 625 (2000).
  - <sup>13</sup>J. C. Gómez Sal, N. Marcano, J. I. Espeso, J. Hernández Velasco, and B. Farago, *Physica B* **385–386**, 372 (2006).
  - <sup>14</sup>N. Marcano, G. M. Kalvius, D. R. Noakes, J. I. Espeso, J. C. Gómez Sal, C. Baines, and A. Amato, *Physica B* **374–375**, 17 (2006).
  - <sup>15</sup>N. Marcano, J. C. Gómez Sal, J. I. Espeso, J. M. De Teresa, P. A. Algarabel, C. Paulsen, and J. R. Iglesias, *Phys. Rev. Lett.* **98**, 166406 (2007).
  - <sup>16</sup>S. G. Magalhaes, F. M. Zimmer, P. R. Krebs, and B. Coqblin, *Phys. Rev. B* **74**, 014427 (2006).
  - <sup>17</sup>J. C. Gómez Sal, J. I. Espeso, J. Rodríguez Fernández, N. Marcano, and J. A. Blanco, *J. Magn. Magn. Mater.* **242–245**, 125 (2002).
  - <sup>18</sup>N. Marcano, D. Paccard, J. I. Espeso, J. Allemand, J. M. Moreau, A. Kurbakov, C. Sekine, C. Paulsen, E. Lhotel, and J. C. Gómez Sal, *J. Magn. Magn. Mater.* **272–276**, 468 (2004).
  - <sup>19</sup>B. Dieny and B. Barbara, *Phys. Rev. Lett.* **57**, 1169 (1986).
  - <sup>20</sup>S. Mukherjee, R. Ranganathan, P. S. Anilkumar, and P. A. Joy, *Phys. Rev. B* **54**, 9267 (1996).
  - <sup>21</sup>A. Maignan, C. Martin, F. Damay, B. Raveau, and J. Hejtmanek, *Phys. Rev. B* **58**, 2758 (1998).
  - <sup>22</sup>J. García Soldevilla, J. C. Gómez Sal, J. Rodríguez Fernández, J. I. Espeso, L. Monconduit, J. Allemand, and D. Paccard, *Physica B* **230–232**, 117 (1997).
  - <sup>23</sup>L. Fernández Barquín, J. C. Gómez Sal, P. Gorria, J. S. Garitaonandia, and J. M. Barandiarán, *Eur. Phys. J. B* **35**, 3 (2003).
  - <sup>24</sup>T. Nishioka, Y. Tabata, T. Taniguchi, and Y. Miyako, *J. Phys. Soc. Jpn.* **69**, 1012 (2000).
  - <sup>25</sup>S. Süllo, G. J. Nieuwenhuys, A. A. Menovsky, J. A. Mydosh, S. A. M. Mentink, T. E. Mason, and W. J. L. Buyers, *Phys. Rev. Lett.* **78**, 354 (1997).
  - <sup>26</sup>D. X. Li, T. Yamamura, S. Nimori, K. Yubuta, and Y. Shiokawa, *Appl. Phys. Lett.* **87**, 142505 (2005).
  - <sup>27</sup>E. M. Levin, V. K. Pecharsky, and K. A. Gschneidner, Jr., *J. Appl. Phys.* **90**, 6255 (2001).
  - <sup>28</sup>C. C. Paulsen, S. J. Williamson, and H. Maletta, *Phys. Rev. Lett.* **59**, 128 (1987).
  - <sup>29</sup>J. L. Tholence, *Solid State Commun.* **35**, 113 (1980).
  - <sup>30</sup>J. Souletie and J. L. Tholence, *Phys. Rev. B* **32**, 516 (1985).
  - <sup>31</sup>A. T. Ogielski and I. Morgenstern, *Phys. Rev. Lett.* **54**, 928 (1985).
  - <sup>32</sup>S. Geschwind, D. A. Huse, and G. E. Devlin, *Phys. Rev. B* **41**, 4854 (1990).
  - <sup>33</sup>M. A. López de la Torre, J. Rodríguez Fernández, K. A. McEwen, and M. B. Maple, *Phys. Rev. B* **74**, 014431 (2006).
  - <sup>34</sup>D. P. Rojas, L. Fernández Barquín, J. Rodríguez Fernández, J. I. Espeso, and J. C. Gómez Sal, *J. Phys.: Condens. Matter* **19**, 186214 (2007).
  - <sup>35</sup>E. M. Chudnovsky, *J. Appl. Phys.* **64**, 5770 (1988).
  - <sup>36</sup>A. Caneschi, T. Ohm, C. Paulsen, D. Royal, C. Sangregorio, and R. Sessolia, *J. Magn. Magn. Mater.* **177–181**, 1330 (1998).
  - <sup>37</sup>R. Mahendiran, A. Maignan, S. Hébert, C. Martin, M. Hervieu, B. Raveau, J. F. Mitchell, and P. Schiffer, *Phys. Rev. Lett.* **89**, 286602 (2002).
  - <sup>38</sup>J. R. Friedman, M. P. Sarachik, J. Tejada, and R. Ziolo, *Phys. Rev. Lett.* **76**, 3830 (1996).
  - <sup>39</sup>See, for instance, V. Hardy, S. Majumdar, M. R. Lees, D. McK. Paul, C. Yaicle, and M. Hervieu, *Phys. Rev. B* **70**, 104423 (2004).
  - <sup>40</sup>J. M. D. Coey, T. R. McGuire, and B. Tissier, *Phys. Rev. B* **24**, 1261 (1981).
  - <sup>41</sup>L. D. Tung, *Phys. Rev. B* **72**, 054414 (2005).
  - <sup>42</sup>R. Iglesias *et al.* (unpublished).
  - <sup>43</sup>E. Lhotel, C. Paulsen, and A. D. Huxley, *Phys. Rev. Lett.* **91**, 209701 (2003); *J. Magn. Magn. Mater.* **272–276**, 179 (2004).
  - <sup>44</sup>G. Alejandro, L. B. Steren, A. Caneiro, J. Cartes, E. E. Vogel, and P. Vargas, *Phys. Rev. B* **73**, 054427 (2006).